A Rotating Restart Method for Scalar (v/f) Controlled Synchronous Reluctance Machine Drives Using a Single DC-Link Current Sensor

KIBOK LEE [1], **(Member, IEEE), HEONYOUNG KIM**[2], **(Student Member, IEEE), AND SRDJAN M. LUKIC**[2], **(Senior Member, IEEE)**

[1]Department of Mechatronics Engineering, Incheon National University, Incheon 22012, South Korea
[2]Department of Electrical and Computer Engineering, North Carolina State University, Raleigh, NC 27606, USA

Corresponding author: Kibok Lee (kibok.lee@inu.ac.kr)

ABSTRACT This paper presents a rotating restart method for *v/f* scalar controlled Synchronous Reluctance Machines (SynRMs) using a single *DC*-link current sensor. In such a case, the initial rotor position and speed are required to restart the machine due to the absence of a position sensor. The method proposes to inject three active voltage vectors in the stationary reference frame to induce the phase currents required for estimating the rotor position and speed. In addition, the phase current reconstruction method is proposed to reduce the distortion of the measured phase currents caused by adopting a single *DC*-link current sensor and to consequently enhance the rotor position estimation accuracy. With the proposed method, the appropriate voltage vector can be applied to the machine, thus minimizing the inrush current during the restart. Furthermore, the proposed method only requires the machine parameters on the nameplate, and it does not require any additional machine-specific tuning processes. This paper proposes a simple restart method suitable for scalar-controlled SynRM drives with a single *DC*-link current sensor. The effectiveness of the proposed restart scheme is validated through the simulation and experimental results.

INDEX TERMS Synchronous reluctance motor (SynRM), restart method, rotor position and speed estimation, scalar (V/f) control, single DC-link current sensor.
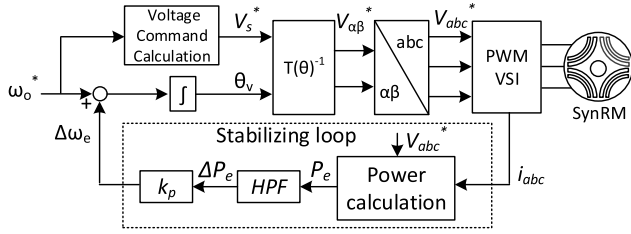
I. INTRODUCTION

Industrial machines are typically started from the zero speed regardless of the control methods. However, in some cases, the machine is rotating before being fed by the inverter due to the momentary power interruptions or the delivered torque from the external load. If the voltage is applied from the zero frequency while the rotor is rotating, an overcurrent trip can occur due to both the voltage and the frequency mismatch. Especially, this is a serious problem in many applications with large shaft inertia because it may take several minutes for the machine to stop completely. In such cases, a flying restart would be a beneficial strategy to improve the productivity and time efficiency in industrial applications, as the machines can be started without waiting for them to reach the zero speed.

The associate editor coordinating the review of this manuscript and approving it for publication was Atif Iqbal [ID].

Three-phase voltage source inverters have been widely used in variable frequency drive applications. In such systems, the motor current feedback signals are essential for the control systems, and two or three current sensors are usually required. However, the use of sensors generally increases the cost, volume, weight, and complexity. In low-cost drive systems, such as fans or pumps, the use of sensors should be minimized. Therefore, the control strategies of drive systems that use a single *DC*-link current sensor have been intensively investigated [1]–[5]. In addition, the use of a single *DC*-link current sensor removes the undesirable unbalance of the three-phase currents caused by the *DC*-offset and the gain sensitivity of the phase current sensors [3]. This work focuses on the inverter systems only using a single *DC*-link current sensor to drive *AC* machines.

Recently, SynRMs have been widely used in many industrial applications, as they offer higher power density and efficiency in comparison with induction machines (IMs),

and they also cost less than permanent magnet synchronous machines (PMSMs) [6], [7]. Moreover, SynRMs are controlled in *v/f* mode in many applications that do not require high dynamic performance, such as fans or pumps, so as to ensure easier commissioning by the end-users [8], [9]. The *v/f* scalar control only requires a few machine parameters, such as the machine rating and the *V-f* ratio.

The goal of this work is to develop a restart method for scalar-controlled SynRMs that drive high inertia loads using a single *DC*-link current sensor. Various methods for estimating the machine speed have been proposed for IMs [10]–[17]. The proposed approach in [10]–[15] uses a frequency search method relying on the slip information because the stator current is minimized when the searching frequency reaches the rotor rotational speed. However, these methods are not suitable for SynRMs because the rotor current is not conducted in SynRMs. The approach in [16], [17] utilizes an adaptive flux observer and requires the *DC* current injection to estimate the rotor rotational speed. However, these methods require accurate machine parameter information and current controllers.

In the case of PMSMs, an approach in [18]–[22] was recently proposed for estimating the machine speed and position. These PMSM restart methods inject zero-voltage pulses to extract information about the rotor position from the current vector induced by the back electromotive force (EMF). However, this voltage injection method cannot be applied to restart SynRMs, as zero-voltage pulses do not induce the stator current. In SynRMs, if the current is not flowing through the stator winding, the back-EMF is not induced due to the absence of permanent magnets in the rotor even if the machine is rotating.

The high-frequency signal injection method can be used as an alternative method to estimate the rotor rotational speed and position [23]–[29], and it can accurately estimate the rotor position and speed even when the speed is near zero. However, this method requires the complex signal demodulation process to extract the rotor position information and the machine-specific tuning to maintain the constant bandwidth of the state filter or the observer. Therefore, it would sacrifice the simplicity of scalar control and increase the complexity of the restart algorithm. The method in [30] injects v_1 active voltage pulses to induce the stator current, and the rotor position angle and speed are extracted from the induced stator current. This method only requires information on the motor nameplate and the three-phase currents that are measured by the phase current sensors in the inverter. However, if the inverter system only uses a single *DC*-link current sensor to measure the machine current, the three-phase currents cannot be simultaneously measured with one active voltage vector during a single switching period. Therefore, the method in [30] is not applicable for inverter systems that only use a single *DC*-link current sensor. A restart method for SynRM drive systems that only uses a single *DC*-link current sensor was proposed in [31]; however, this method has a significant

FIGURE 1. Equivalent circuit of the SynRM in the rotor reference frame; (a) d-axis circuit (b) q-axis circuit.

FIGURE 2. Phasor diagram of the *v/f* controlled SynRM in the steady-state.

position estimation error because of the used current sampling method.

This paper presents a restart method that injects three active voltage vectors to measure three-phase currents by using a single *DC*-link current sensor. The paper also proposes a current reconstruction algorithm to reduce the distortion of the phase currents measured by the *DC*-link current sensor and to consequently enhance the accuracy of the rotor position and speed estimation. The detailed implementation method is provided, and the simulation and experimental results are presented to verify the performance of the proposed approach.

II. SCALAR CONTROL FOR SynRM DRIVE

From Fig. 1, the equation describing the electrical dynamics of SynRM machines in the rotor reference frame can be represented as follows [29]:

$$\begin{bmatrix} v_d^r \\ v_q^r \end{bmatrix} = \begin{bmatrix} r_s + pL_d & -\omega_r L_q \\ \omega_r L_d & r_s + pL_q \end{bmatrix} \begin{bmatrix} i_d^r \\ i_q^r \end{bmatrix}, \quad (1)$$

where p is the derivative operator, r_s is the stator winding resistance, v_d^r and v_q^r are the *d-q* axis stator input voltages in the synchronous reference frame, i_d^r and i_q^r are the *d-q* axis stator currents in the rotor reference frame, L_d and L_q are the *d-q* axis stator inductances, and ω_r is the rotor's electrical speed.

In the *v/f* control, the γ-δ axis synchronous reference frame is generally used for the control, where the δ-axis is aligned with the stator voltage vector. Only the amplitude and the frequency of the voltage vector are controlled without the information of the rotor position; therefore, the *v/f* control can easily be implemented compared to the vector control. Fig. 2 shows the phasor diagram of the stator voltage and

FIGURE 3. Conventional v/f closed-loop control scheme with a stabilizing loop.

FIGURE 4. Applying v_1, v_3, and v_5 voltage vectors in the stationary reference frame.

current vectors in the γ-δ and d-q synchronous reference frames. The magnitude of the voltage command V_s in the v/f control is determined to maintain the constant stator flux linkage λ_s so as to have the same torque capability in all operating ranges [8], [9]. E_s is the voltage induced by the stator flux linkage. The stator command voltage can be instantaneously calculated as [9]:

$$V_s^* = r_s I_s \cos\varphi + \sqrt{\left(\omega_0 \frac{V_{rated}}{\omega_{rated}}\right)^2 + (r_s I_s \cos\varphi)^2 - (r_s I_s)^2}, \quad (2)$$

where ω_0 is the speed command, V_{rated} is the rated voltage, ω_{rated} is the rated speed, I_s is the magnitude of the current vector, and φ is the power factor. The magnitude of the current vector can be calculated from the three-phase currents measured by the *DC*-link current sensor [1]–[5]. In (2), the stator resistance voltage drop is compensated to maintain a constant flux. Also, the term $I_s \cos\varphi$ can be instantaneously calculated as:

$$I_s \cos\varphi = \frac{2}{3}\left[i_{as}\cos\theta_v + i_{bs}\cos\left(\theta_v - \frac{2\pi}{3}\right) + i_{cs}\cos\left(\theta_v + \frac{2\pi}{3}\right)\right] \quad (3)$$

where θ_v is the position angle of the stator voltage vector in the stationary reference frame.

The open-loop v/f control of SynRM easily loses synchronization under load disturbances, as the synchronous motor is inherently unstable due to the absence of damper windings [8], [9]. Therefore, the v/f control for SynRMs requires a stabilizing feedback loop to ensure stable operation. Fig. 3 shows the conventional v/f control method with a stabilizing loop [9]. The frequency modulation signal $\Delta\omega_e$ is generated in the stabilizing loop to tolerate the load disturbance. In the stabilizing loop, the calculated input power passes through the high-pass filter to extract the power perturbation ΔP_e. The proportional gain k_p is properly selected to place the system poles in the stable region [9].

III. PROPOSED RESTART METHOD

This work aims to develop a restart algorithm suitable for scalar controlled SynRM drives using a single *DC*-link current sensor. The initial rotor position and speed are required to restart the motor in the free-running state. This section describes how the proposed method estimates the rotor position and speed during the free running of the rotor.
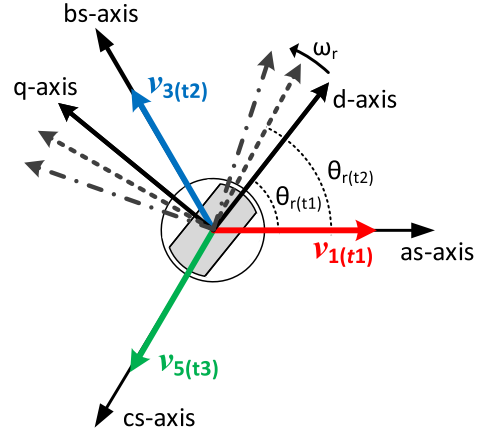
A. APPLYING ACTIVE VOLTAGE PULSES

The proposed method basically excites the machine with v_1, v_3, and v_5 voltage vector pulses to measure the resulting stator current. In Fig. 4, v_1, v_3, and v_5 voltage vectors are applied in sequence at times t_1, t_2, and t_3, respectively, and this voltage injection process is continuously repeated while estimating the rotor position and speed of the motor in the free-running state. When applying active voltage vector pulses to a machine, the pulse time (t_{pulse}) of the applied voltages is assumed to be much shorter than the stator time constants ($\tau_d = L_d/r_s$, $\tau_q = L_q/r_s$). Thus, the stator resistance r_s can be neglected, and the induced current by the applied voltage pulse can be expressed by simplifying (1) as:

$$p\begin{bmatrix} i_d^r \\ i_q^r \end{bmatrix} = \begin{bmatrix} 0 & \omega_r L_q/L_d \\ -\omega_r L_d/L_q & 0 \end{bmatrix}\begin{bmatrix} i_d^r \\ i_q^r \end{bmatrix} + \begin{bmatrix} v_d^r/L_d \\ v_q^r/L_q \end{bmatrix} \quad (4)$$

The active voltage vectors applied to excite the machine can be expressed in the synchronous rotor reference frame as:

$$v_d^r = \frac{2V_{dc}}{3}\cos\left(\frac{\pi}{3}(n-1) - \theta_r\right)$$
$$v_q^r = \frac{2V_{dc}}{3}\sin\left(\frac{\pi}{3}(n-1) - \theta_r\right) \quad (5)$$

Here, V_{dc} is the *DC*-link voltage of the voltage source inverter (*VSI*), θ_r is the actual electric rotor angle, and n is the number of the applied voltage vectors ($n = 1, 3, 5$). When the voltage vector v_1 is injected to the machine, the d-q axis voltage can be expressed as:

$$v_d^r = \frac{2V_{dc}}{3}\cos\theta_r$$
$$v_q^r = -\frac{2V_{dc}}{3}\sin\theta_r \quad (6)$$

Since the machine is driving a high inertia load, the rotor speed ω_r can be assumed constant. Thus, the d-q axis current in the rotor reference frame that is driven by the voltage

vector v_1 can be obtained by solving (4) through the Laplace transform:

$$i_d^r(t_{pulse})$$
$$= \frac{2V_{dc}}{3} \frac{(\cos(\omega_r t_{pulse}) - 1)\sin(\theta_r) + \sin(\omega_r t_{pulse})\cos(\theta_r)}{\omega_r L_d}$$
$$i_q^r(t_{pulse})$$
$$= \frac{2V_{dc}}{3} \frac{(\cos(\omega_r t_{pulse}) - 1)\cos(\theta_r) - \sin(\omega_r t_{pulse})\sin(\theta_r)}{\omega_r L_q}$$
$$\tag{7}$$

where t_{pulse} is the applied pulse time of the voltage v_1. The initial state of the d-q axis currents is zero because the machine is in the free-running state. Since t_{pulse} is short enough, $\cos(\omega_r t_{pulse})$ and $\sin(\omega_r t_{pulse})$ can be considered, respectively, as 1 and $\omega_r t_{pulse}$. Then, the d-q axis current of (7) can then be simplified as:

$$i_d^r(t_{pulse}) = \frac{2V_{dc}t_{pulse}}{3}\frac{\cos(\theta_r)}{L_d}$$
$$i_q^r(t_{pulse}) = -\frac{2V_{dc}t_{pulse}}{3}\frac{\sin(\theta_r)}{L_q} \tag{8}$$

From (8), the induced current in the proposed method does not depend on the rotor speed. The d-q axis current can be transformed using the inverse Park's transformation to three-phase currents in the stationary reference frame as:

$$i_a = \frac{V_{dc}t_{pulse}}{3}\left(\left(\frac{1}{L_d} + \frac{1}{L_q}\right) + \left(\frac{1}{L_d} - \frac{1}{L_q}\right)\cos(2\theta_r)\right);$$
$$i_b = \frac{V_{dc}t_{pulse}}{3}\left(-\frac{1}{2}\left(\frac{1}{L_d} + \frac{1}{L_q}\right) + \left(\frac{1}{L_d} - \frac{1}{L_q}\right)\cos\left(2\theta_r - \frac{2\pi}{3}\right)\right);$$
$$i_c = \frac{V_{dc}t_{pulse}}{3}\left(-\frac{1}{2}\left(\frac{1}{L_d} + \frac{1}{L_q}\right) + \left(\frac{1}{L_d} - \frac{1}{L_q}\right)\cos\left(2\theta_r + \frac{2\pi}{3}\right)\right) \tag{9}$$

The three-phase currents in (9) consist of two terms. The first term is the *DC*-offset current, and the second term is the oscillated portion with respect to the rotor position. The rotor position can be estimated by extracting the *AC* term from the induced stator current. Also, it can be noted that the frequency of the *AC* current is two times faster than the rotor electrical frequency.

B. ROTOR POSITION AND SPEED ESTIMATION
This work focuses on developing the restart method by only using a *DC*-link current sensor without using phase current sensors. In such a case, the three-phase currents cannot be simultaneously measured while estimating the rotor position and speed. Thus, v_1, v_3, and v_5 voltage pulses are applied in sequence to measure the three-phase currents as shown in Fig. 5. When an active voltage v_1 is applied to the machine at t_1, the phase a current is measured by the *DC*-link current sensor [1]–[5]. Then, the measured phase a current is held until the next v_1 voltage is applied at t_4. Similarly, the phase b and c currents are respectively measured when the v_3 and the v_5 voltage pulses are applied. t_{sw} is the switching period
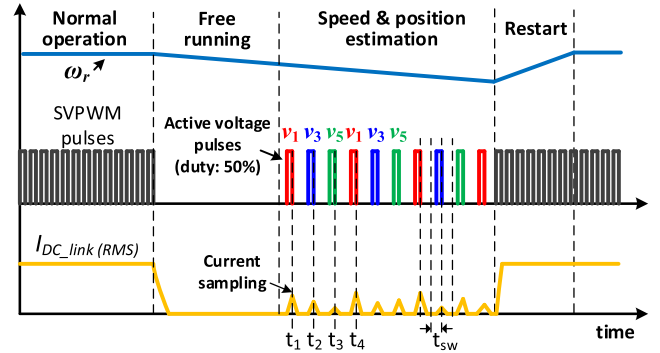
FIGURE 5. Conceptual diagram of the restart method using active voltage pulses.
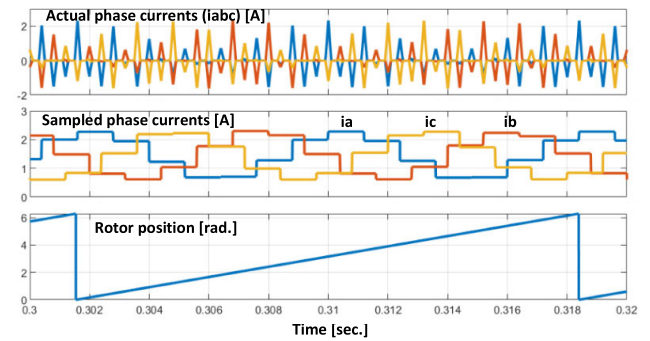
FIGURE 6. The actual and sampled three-phase currents caused by v_1, v_3, and v_5 voltage pulses in the estimation mode.

TABLE 1. SynRM motor parameters.

Parameter	Unit	Symbol	Values
Rated Power	[kW]	P_{out}	18
Rated Speed	[rpm]	N_r	1800
Rated Torque	[Nm]	T_e	95
Rated Voltage (line-line)	[V]	V_s	380
Rated Phase Current	[Arms]	i_s	33
Pole	-	n	4
Stator Resistance	[Ω]	R_s	0.19
Stator d-axis Inductance	[mH]	L_d	57
Stator q-axis Inductance	[mH]	L_q	15
Inertia	[Nm/rad·s^{-2}]	J	0.06
PWM Switching Period	[μsec]	t_{sw}	200

of the inverter. The active voltage pulses are injected every two switching periods to induce the current from zero. This is because the initial state of the stator current is zero when deriving the induced current in (7)–(9). This method can also use v_2, v_4, and v_6 voltage vector pulses to measure the three-phase currents. For example, when v_2 voltage pulse is applied, the *DC*-link current in the inverter is equal to the negative value of phase c current.

Fig. 6 shows the simulation results of the three-phase currents in the estimation mode when the v_1, v_3, and v_5 voltage vectors are applied to the machine in consecutive order. The machine parameters used for the simulation are listed in Table 1. The rotor speed in the simulation is 1,800 rpm, and the applied voltage pulse duty cycle is 50%. The figure on the top shows the actual discontinuous three-phase currents

induced by the voltage pulses, the second waveforms show the sampled three-phase currents that are updated at the end of each applied voltage pulse as shown in Fig. 5, and the bottom one shows the actual rotor position. The sampled three-phase currents have a negative sequence although v_1, v_3, and v_5 are applied in a positive sequence. The resulting three-phase currents by the v_1, v_3, and v_5 voltage vector pulses are expressed as:

$$i_a(t_1) = \frac{V_{dc}t_{pulse}}{3}\left(\frac{1}{L_d}+\frac{1}{L_q}+\left(\frac{1}{L_d}-\frac{1}{L_q}\right)\cos\left(2\theta_{r(t1)}\right)\right);$$

$$i_b(t_2) = \frac{V_{dc}t_{pulse}}{3}\left(\frac{1}{L_d}+\frac{1}{L_q}+\left(\frac{1}{L_d}-\frac{1}{L_q}\right)\cos\left(2\theta_{r(t2)}+\frac{2\pi}{3}\right)\right);$$

$$i_c(t_3) = \frac{V_{dc}t_{pulse}}{3}\left(\frac{1}{L_d}+\frac{1}{L_q}+\left(\frac{1}{L_d}-\frac{1}{L_q}\right)\cos\left(2\theta_{r(t3)}-\frac{2\pi}{3}\right)\right)$$

(10)

where i_a, i_b, and i_c are the induced currents at t_1, t_2, and t_3, respectively. As previously mentioned, the controller holds each sampled phase current value until the next instant of applying the same voltage vector. The three-phase currents measured at t_1, t_2, and t_3 are used to estimate the rotor position in every switching period. Before estimating the rotor position, the DC-offset terms in (10) should be removed from the measured three-phase currents. The DC-offset current can be obtained by averaging the three-phase currents for several periods of the machine fundamental frequency. Then, the AC current terms (i_{a_AC}, i_{b_AC}, and i_{c_AC}) are calculated by subtracting the DC-offset from the measured three-phase currents as:

$$i_{a\_AC}(t_1) = I_{mag}\cos\left(2\theta_{r(t1)}\right);$$

$$i_{b\_AC}(t_2) = I_{mag}\cos\left(2\theta_{r(t2)}+\frac{2\pi}{3}\right);$$

$$i_{c\_AC}(t_3) = I_{mag}\cos\left(2\theta_{r(t3)}-\frac{2\pi}{3}\right)$$

(11)

Here, I_{mag} is the amplitude of the current, and it can be presented as $V_{dc} \cdot t_{pulse}/3 \cdot (1/L_d - 1/L_q)$. With the Clarke transformation, the α-β axis currents $i^s_{\alpha\_AC}$ and $i^s_{\beta\_AC}$ in the stationary reference frame can be obtained. As a result, the rotor position can be estimated by injecting the active voltage pulses as:

$$\theta_{est} = \theta_r + \Delta\theta_{error} = \frac{1}{2}tan^{-1}\left(\frac{i^s_{\beta\_AC}}{i^s_{\alpha\_AC}}\right)$$

(12)

where θ_{est} is the estimated rotor angle, θ_r is the actual rotor angle, and $\Delta\theta_{error}$ is the error term of the estimated rotor angle. The estimated position angle inherently has an estimation error due to the way it samples and holds the motor current. This error increases with the increase in the rotor speed due to the limited samples of the current measurements.

The current reconstruction method is introduced to reduce the error in the rotor position estimation. The difference in the instantaneous phase a current between the two sequential switching periods can be defined as:

$$\Delta i_{a\_AC} = I_{mag}\cos\left(\theta_I + \omega_I t_{sw}\right) - I_{mag}\cos\theta_I \quad (13)$$
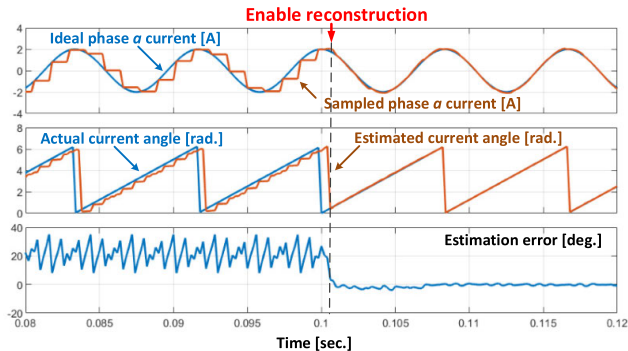
FIGURE 7. Simulation results of the current vector angle estimation without and with the proposed current reconstruction method.

where θ_I and ω_I are the estimated angle and the estimated speed of the current vector in (11), respectively. As previously mentioned, the rotational speed ω_I of the current vector is two times faster than the rotor electrical speed ω_r. I_{mag} is the phase current magnitude, and it can be calculated from the α-β axis currents $i^s_{\alpha\_AC}$ and $i^s_{\beta\_AC}$. Since t_{sw} is short enough, $\cos(\omega_I t_{sw})$ and $\sin(\omega_I t_{sw})$ can be respectively considered as 1 and $\omega_I t_{sw}$. Then, (13) can be simplified as:

$$\Delta i_{a\_AC} = -I_{mag}\omega_I t_{sw}\sin\theta_I \quad (14)$$

The phase a current is reconstructed using (14) with the estimated current angle, speed, and magnitude until the next v_1 voltage pulse is applied to the machine. In the same way, this reconstruction method can be applied to the phase b and c currents. The three-phase currents are only reconstructed with the following when each phase current is not updated with the DC-link current sensor.

$$i_{a\_AC}[k] = i_{a\_AC}[k-1] - I_{mag}\omega_I t_{sw}\sin\theta_I$$

$$i_{b\_AC}[k] = i_{b\_AC}[k-1] - I_{mag}\omega_I t_{sw}\sin\left(\theta_I + 2\pi/3\right)$$

$$i_{c\_AC}[k] = i_{c\_AC}[k-1] - I_{mag}\omega_I t_{sw}\sin\left(\theta_I - 2\pi/3\right) \quad (15)$$

where k indicates the current switching period and k-1 indicates the previous switching period.

Fig. 7 shows the simulation results of the current vector angle estimation when the proposed current reconstruction method is used. The rotor speed in this simulation is 1,800 rpm. The top plot shows the sampled phase a current at every six switching periods as shown in Fig. 5. The ideal phase a current is also plotted to clearly demonstrate the distortion of the sampled phase current. The second plot shows the actual current vector position and the current vector position estimated from the sampled three-phase currents. The bottom plot shows the error of the estimated current vector position. In the left half region, the phase current is updated every six switching periods, and the current reconstruction method is not used. This phase current distortion causes a significant error in the estimation of the current vector position. The maximum estimation angle error of the current vector position is about 30 [deg.] at this speed, which may cause a restart failure due to the inrush current at the
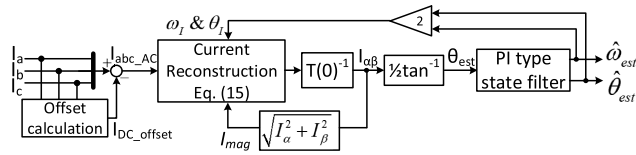
FIGURE 8. Block diagram for estimating the rotor position angle and the rotor speed while using the phase current reconstruction.
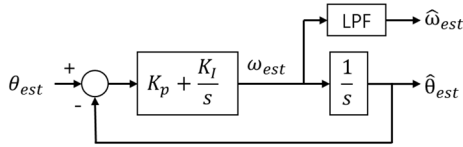

FIGURE 9. Block diagram of the PI type state filter for filtering the estimated rotor position angle and estimating the rotor speed.
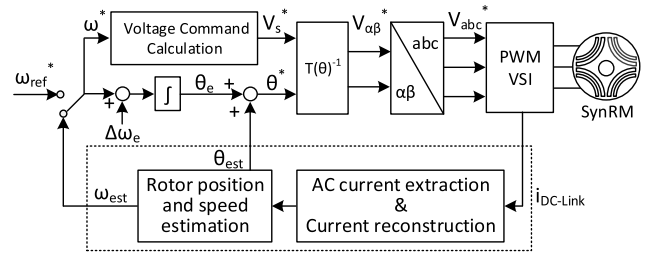

FIGURE 10. Complete scalar (v/f) control scheme for SynRMs with the proposed restart method.

FIGURE 11. Schematic of an Inverter with a DC-link current sensor.

instant of restarting. In the right half region, the current reconstruction method is used. The phase current is updated every six switching periods with the current measured with the DC-link current sensor, and the phase current is reconstructed every switching period using (15). The distortion of the phase current is significantly reduced. As a result, the accuracy of the position estimation is enhanced.

Fig. 8 shows the proposed block diagram for estimating the rotor position angle and the rotor speed while using the phase current reconstruction. The estimated rotor position angle passes through the PI type state filter to minimize the estimation error. The transfer function of the PI type state filter is as follows:

$$\frac{\hat{\theta}_{est}}{\theta_{est}} = \frac{K_p s + K_I}{s^2 + K_P s + K_I} \tag{16}$$

The gains are set to place all the closed-loop eigenvalues at 100 rad/s.

The rotor speed can be estimated by the PI type state filter as shown in Fig. 9, and the additional low-pass filter (LPF) is used to reduce the ripple of the speed extracted from the state filter. The cutoff frequency of the LPF is selected as 10 Hz. The estimated speed, which passes through the LPF, is used to reconstruct the phase currents and restart the machine. The delay of position and speed estimation caused by the PI type state filter and the LPF is negligible because the rotor speed variation is almost constant, as the machine drives a high inertia load.

C. IMPLEMENTATION OF THE PROPOSED RESTART METHOD

Fig. 10 shows the proposed complete scheme for restarting the SynRM. In the normal operation mode, the machine is controlled with the v/f scalar control with the modulation frequency $\Delta\omega_e$ to ensure stable operation in all the operating ranges [9]. The controller is set with the motor nameplate parameters, and the drive system only uses a single DC-link current sensor. When a restart is required, the rotor position and speed of the free-running motor are estimated with the three-phase current measured by the DC-link current sensor. The dotted block is the proposed part that was
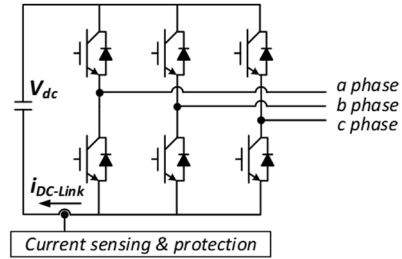
shown in Fig. 8 for the rotor position and speed estimation. Fig. 11 shows the schematic of a 3-phase inverter with a single DC-link current sensor.

The procedure for implementing the proposed restart method is explained in this section. First, the voltage vectors v_1, v_3, and v_5 are applied to the machine, which maintains its free-running state due to the high inertia load. The initial duty of the applied voltage is set to 50%. The magnitude of the phase current induced by the v_1, v_3, and v_5 voltage pulses is calculated using (8) as:

$$I_s = \frac{2V_{dc}t_{pulse}}{3}\left(\frac{\cos(\theta_r)^2}{L_d^2} + \frac{\sin(\theta_r)^2}{L_q^2}\right)^{1/2} \tag{17}$$

where I_s is the magnitude of the phase current vector. At this point, it should be noted that this current magnitude cannot be calculated before applying the voltage pulses because the d-q axis inductance is not generally listed on the motor nameplate. From (17), if the DC-link voltage is too high or the applied voltage pulse time is too long, an undesired overcurrent can take place. Therefore, a strategy for adjusting the pulse duty is proposed using the measured current magnitude and the machine current rating. If the magnitude of the phase current that is induced by the first voltage pulse exceeds the level of the rated current, the new pulse duty is calculated as:

$$t_{pulse\_new} = \frac{I_{rated}/10}{I_s}t_{pulse} \tag{18}$$

where I_{rated} is the rated current and I_s is the magnitude of the phase current caused by the first voltage pulse. The new pulse duty is then calculated to induce a much smaller current than the motor rated current. Then, the voltage pulses are applied again with the new pulse duty (t_{pulse_new}).

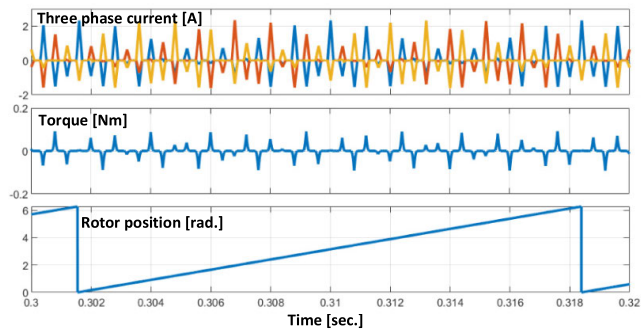Another concern is that the electromagnetic torque is generated by the applied voltage pulses during the estimation

FIGURE 12. Electromagnetic torque generated by the three active voltage vector (v_1, v_3, and v_5) pulses in the estimation mode.
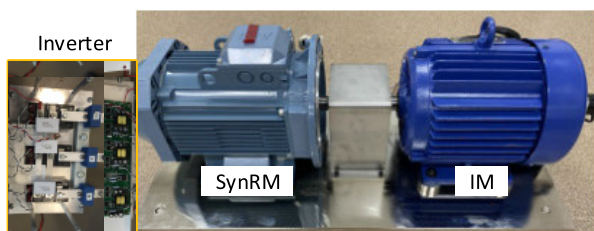

FIGURE 13. Experimental setup of the SynRM drive system.

of the rotor position and speed. The torque equation of the SynRM is given by [29]:

$$T_e = \frac{P}{2}\frac{3}{2}\left(L_d - L_q\right) i_d^r i_q^r \qquad (19)$$

where P is the machine pole number. The torque generated by the current induced by the v_1 voltage pulse is calculated by substituting (8) into (19) as:

$$T_e = \frac{3P}{8}\left(\frac{2V_{dc}t_{pulse}}{3}\right)^2\left(\frac{1}{L_d} - \frac{1}{L_q}\right)\sin\left(2\theta_r\right) \qquad (20)$$

Similarly, when the v_3 and v_5 voltage pulses are applied, the magnitude of the generated torque is the same as in (20). This resulting torque is negligible if the voltage pulse time, which mainly depends on the switching period, is sufficiently short. In addition, the average torque generated for a single revolution is zero; therefore, it does not cause a high braking torque. Fig. 12 shows the simulation results when applying the voltage pulses to the machine in the estimation mode. The rotor speed in this simulation is 1,800 rpm, and the applied voltage pulse duty cycle is 50%. The top plot shows the actual three-phase currents, the second plot shows the torque generated by the induced current, and the bottom plot shows the actual rotor position while injecting the active voltage pulses.

Next, the induced phase currents are averaged to calculate the *DC*-offset component, which is essential for extracting the three *AC* current terms (i_{abc_AC}). With the extracted *AC* current terms, the rotor position and speed are estimated.

The estimated position angle (θ_{est}) is aligned with the d-axis in the rotor reference frame. The angle should be compensated for the voltage to be applied to the q-axis so as to ensure a positive electric torque at the restart instant.

The compensated angle (θ_{comp}) is given by:

$$\theta_{comp} = \theta_{est} + \frac{\pi}{2} + \frac{3}{2}\omega_{est}t_{sw} \qquad (21)$$

By adding $\pi/2$ to θ_{est}, the estimated angle can be aligned to the q-axis. The third term in (21) is to compensate for the current sampling delay ($\omega_{est}t_{sw}$) and the switching period delay ($\omega_{est}t_{sw}/2$) [22], and t_{sw} is the PWM switching period. When the stator voltage ($V_q^r = V$ and $V_d^r = 0$) is applied to the q-axis, the resulting d-q axis current is calculated from (4) as:

$$i_d^r(t_{pulse}) = \frac{V}{\omega_r L_d}(1 - \cos(\omega_r t_{pulse}))$$
$$i_q^r(t_{pulse}) = \frac{V}{\omega_r L_q}\sin(\omega_r t_{pulse}) \qquad (22)$$

The d-q axis current in the rotor reference frame is always positive at the restart instant if the pulse time is short enough.

Finally, the stator voltage is applied to restart the motor. The voltage magnitude is gradually increased from zero to avoid the inrush current, and the applied voltage frequency is fixed to the estimated rotor electrical speed. When the magnitude of the voltage reaches the rated *v/f* value, the increase is stopped.
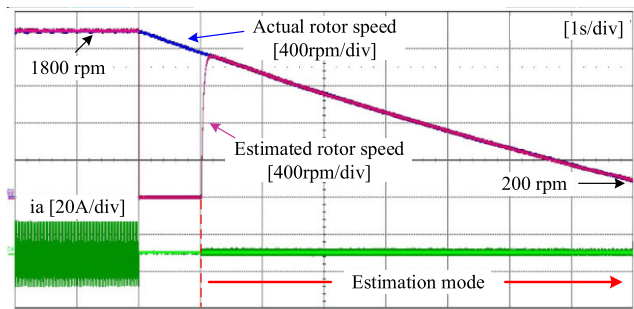
IV. EXPERIMENTAL RESULTS

Experiments were conducted to validate the performance of the proposed restart method. In Fig. 13, the dynamo testbed consists of the tested SynRM and an induction motor as a load machine. The SynRM parameters are given in Table 1. The *VSI* used for driving the test motor includes both phase current sensors and a *DC*-link current sensor. However, a *DC*-link current sensor is only used to implement the proposed restart method. The phase current sensors are used for validating the proposed restart method by monitoring the actual current. The load motor is fed by another commercial *VSI*.

The experimental results in Fig. 14 demonstrate the effectiveness of the current reconstruction method in reducing the current distortion caused by using the *DC*-link current sensor in the estimation mode, thus enhancing the accuracy of rotor position estimation. An encoder sensor is used to only monitor the actual rotor position so as to validate the proposed current reconstruction method. In the left half region of the plot, the phase a current is updated with the *DC*-link current sensor when the v_1 voltage pulses are applied and the current reconstruction method is not enabled. The blue line is the *AC* current term calculated by subtracting the *DC*-offset from the measured phase a current. The yellow line is the actual rotor position angle θ_{act}, and the purple line is the rotor angle θ_{est} estimated using (11) and (12) with the *AC* current terms of the three-phase currents. From (12), the range of the estimated rotor angle is from $-\pi/2$ to $\pi/2$ because the output of the arctangent function is divided by 2. The estimated rotor angle has a significant error in comparison with the actual rotor position. In the right half region, the phase current is updated every six switching periods by the *DC*-link current sensor, and the phase current is reconstructed every switching period
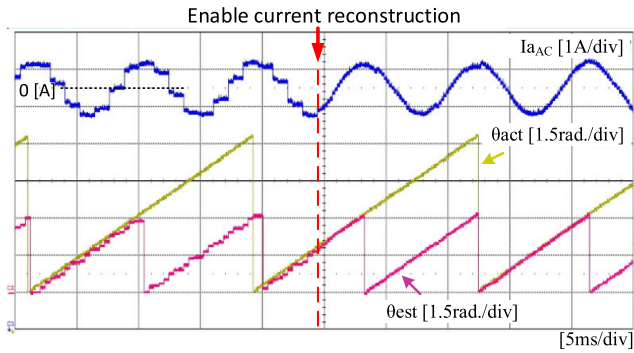
FIGURE 14. Experimental results of the rotor position angle estimation with the current reconstruction method in the estimation mode: the AC current term of the measured phase a current (blue line), the actual rotor angle (yellow line), and the estimated rotor angle (purple line).


FIGURE 15. Experimental results for validating the speed estimation performance of the proposed method: the actual rotor speed (blue line), the estimated rotor speed (purple line), and phase a current (green line).

using (15). The blue line shows the reconstructed phase *a* current. After enabling the proposed current reconstruction method, the phase current distortion is significantly reduced, and the accuracy of the rotor position estimation is enhanced.

Fig. 15 shows the experimental results that validate the performance of the rotor speed estimation method when the rotor speed is reduced. First, the rotor was operating at 1,800 rpm. Next, the inverter was intentionally stopped, and the voltage pulses were applied to estimate the rotor position and speed. The blue line is the actual rotor speed, and the purple line is the estimated rotor speed. The results of this test show that the proposed method has a good performance in terms of speed estimation.
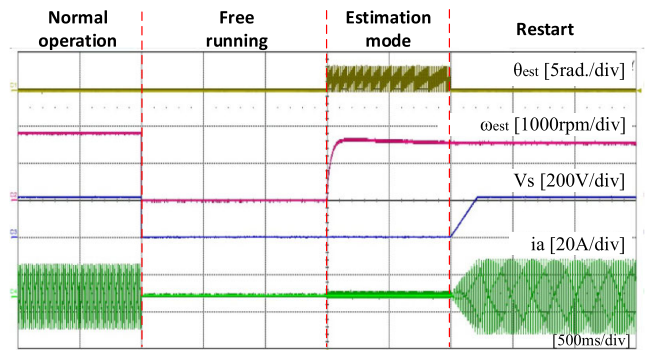
Fig. 16 shows the experimental results of the proposed rotating restart method when the mechanical rotor speed is about 70 rpm, 400 rpm, and 1,600 rpm. The restart tests were implemented with the following steps. The motor was operating at the reference speeds 90 rpm, 450 rpm, and 1,800 rpm. The inverter driving the SynRM was intentionally stopped for 0.3 second in Fig. 16(a). Fig. 16(b) and (c) are the cases when the inverter was stopped for 1.5 seconds. The motor was decelerated due to the influence of friction. Then, the rotor position and speed were estimated by injecting the v_1, v_3, and v_5 voltage pulses, and the motor was again fed by the inverter. The estimation process of the position and speed lasts for 0.7 second in Fig. 16(a) and 1.0 seconds in Fig. 16(b) and (c), respectively. In Fig. 16, the rotor angle (yellow line)
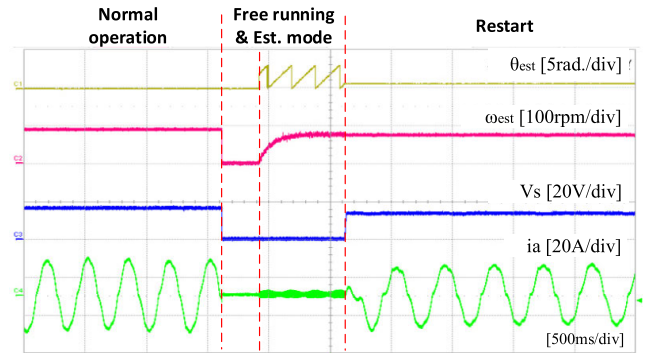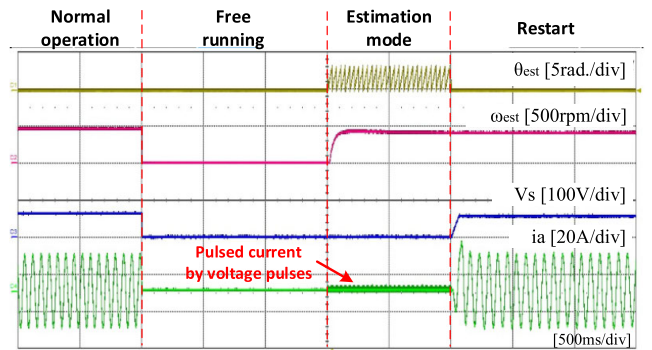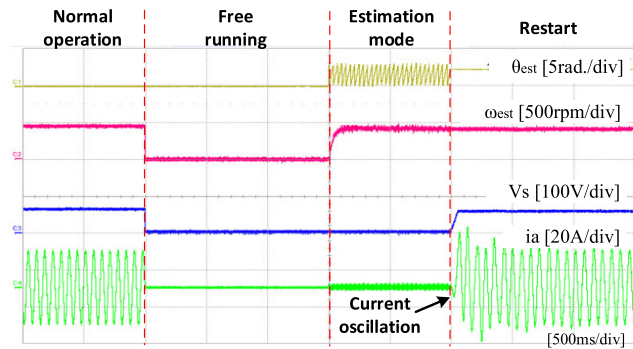

FIGURE 16. Experimental results of the proposed restart method (a) 90 rpm (b) 450 rpm (c) 1,800 rpm: estimated rotor position (yellow line), estimated speed (purple line), magnitude of the stator voltage (blue line), stator phase a current (green line).

and the rotor speed (purple line) were estimated from the measured currents (green line). The blue line plots the applied stator voltage at the restart instant, and the command voltage is calculated from the rated *v/f* ratio. The magnitude of the applied stator voltage was gradually increased from zero to prevent the inrush current. The results of this test verify that the proposed method can successfully estimate the rotor position and speed and that a restart can be implemented without causing inrush currents.

Fig. 17 shows the experimental results of the existing restart method presented in [31] for scalar controlled SynRM drives with a single *DC*-link current sensor. The test was conducted at the rotor speed 450 rpm. In contrast to the proposed method, the existing method does not include the

FIGURE 17. Experimental results of the existing restart method for scalar controlled drives at 450 rpm: estimated rotor position (yellow line), estimated speed (purple line), magnitude of the stator voltage (blue line), stator phase a current (green line).

phase current reconstruction algorithm. This method has a significant rotor position estimation error as shown in the left half region of Fig. 14. This causes larger current oscillations at the restart instant compared to the proposed method in Fig. 16(b).

V. CONCLUSION

This paper presents a restart method suitable for scalar *v/f* controlled SynRM drives with a single *DC*-link current sensor. This study proposes the three active voltage vector injection method to measure the three-phase currents with a *DC*-link current sensor in the estimation mode, and it presents the rotor position and speed estimation method from the induced phase currents. In addition, the proposed current reconstruction algorithm can reduce the distortion of the measured phase currents caused by using the single *DC*-link current sensor and enhance the accuracy of rotor position estimation.

The advantage of the proposed method is that the performance of the rotor speed and position estimation is not affected by the accuracy of the machine parameters because only the ratings listed on the nameplate are necessary for the proposed method. In addition, this method injects voltage pulses in the stationary reference frame and measures only the *DC*-link current. Then, the rotor position information can be extracted by averaging the measured current. Therefore, the proposed method is simpler than the conventional methods that require the complex signal demodulation process and the machine-specific tuning. The performance of the proposed method was verified by the experimental results.

REFERENCES

[1] B. Saritha and P. A. Janakiraman, "Sinusoidal three-phase current reconstruction and control using a DC-link current sensor and a curve-fitting observer," *IEEE Trans. Ind. Electron.*, vol. 54, no. 5, pp. 2657–2664, Oct. 2007.

[2] B. Hafez, A. S. Abdel-Khalik, A. M. Massoud, S. Ahmed, and R. D. Lorenz, "Single-sensor-based three-phase permanent-magnet synchronous motor drive system with luenberger observers for motor line current reconstruction," *IEEE Trans. Ind. Appl.*, vol. 50, no. 4, pp. 2602–2613, Jul. 2014.

[3] H. Kim and T. M. Jahns, "Current control for AC motor drives using a single DC-link current sensor and measurement voltage vectors," *IEEE Trans. Ind. Appl.*, vol. 42, no. 6, pp. 1539–1547, Nov. 2006.

[4] J.-H. Im and R.-Y. Kim, "Improved saliency-based position sensorless control of interior permanent-magnet synchronous machines with single DC-link current sensor using current prediction method," *IEEE Trans. Ind. Electron.*, vol. 65, no. 7, pp. 5335–5343, Jul. 2018.

[5] Y. Gu, F. Ni, D. Yang, and H. Liu, "Switching-state phase shift method for three-phase-current reconstruction with a single DC-link current sensor," *IEEE Trans. Ind. Electron.*, vol. 58, no. 11, pp. 5186–5194, Nov. 2011.

[6] N. Bianchi, S. Bolognani, E. Carraro, M. Castiello, and E. Fornasiero, "Electric vehicle traction based on synchronous reluctance motors," *IEEE Trans. Ind. Appl.*, vol. 52, no. 6, pp. 4762–4769, Nov. 2016.

[7] D. A. Staton, T. J. E. Miller, and S. E. Wood, "Maximising the saliency ratio of the synchronous reluctance motor," *IEE Proc. B-Electr. Power Appl.*, vol. 140, no. 4, pp. 249–259, Jul. 1993.

[8] S.-C. Agarlita, G.-D. Andreescu, C.-E. Coman, and I. Boldea, "Stable V/f control system with controlled power factor angle for permanent magnet synchronous motor drives," *IET Electr. Power Appl.*, vol. 7, no. 4, pp. 278–286, Apr. 2013.

[9] P. D. C. Perera, F. Blaabjerg, J. K. Pedersen, and P. Thogersen, "A sensorless, stable V/f control method for permanent-magnet synchronous motor drives," *IEEE Trans. Ind. Appl.*, vol. 39, no. 3, pp. 783–791, May 2003.

[10] (2017). *Yaskawa High Performance Vector Control Drive Technical Manual.* [Online]. Available: https://www.yaskawa.com

[11] H. Pan, L. Springob, and J. Holtz, "Improving the start and restart behavior through state recognition of AC drives," in *Proc. Power Convers. Conf. (PCC)*, vol. 2, Aug. 1997, pp. 589–594.

[12] H. Iura, K. Ide, T. Hanamoto, and Z. Chen, "An estimation method of rotational direction and speed for free-running AC machines without speed and voltage sensor," *IEEE Trans. Ind. Appl.*, vol. 47, no. 1, pp. 153–160, Jan. 2011.

[13] A. David, E. Lajoie-Mazenc, and C. Sol, "Maintaining the synchronism of an AC adjustable speed drives during short supply interruptions for an optimal and automatic soft restart," in *Proc. Budapest, IEEE Int. Symp. Ind. Electron. Conf. (ISIE)*, Budapest, Hungary, 1993, pp. 463–470.

[14] K. Suzuki, S. Saito, T. Kudor, A. Tanaka, and Y. Andoh, "Stability improvement of V/f controlled large capacity voltage-source inverter fed induction motor," in *Proc. 41st Conf. Rec. IEEE Ind. Appl. Conf. IAS Annu. Meeting*, Oct. 2006, pp. 90–95.

[15] K. Lee, S. Ahmed, and S. M. Lukic, "Universal restart strategy for scalar (V/f) controlled induction machines," *IEEE Trans. Ind. Appl.*, vol. 53, no. 6, pp. 5489–5495, Nov. 2017.

[16] S.-J. Jeong, Y.-M. Park, and G.-J. Han, "An estimation method of rotation speed for minimizing speed variation on restarting of induction motor," in *Proc. 8th Int. Conf. Power Electron. (ECCE) Asia*, May 2011, pp. 697–704.

[17] T. Kikuchi, Y. Matsumoto, and A. Chiba, "Fast initial speed estimation for induction motors in the low-speed range," *IEEE Trans. Ind. Appl.*, vol. 54, no. 4, pp. 3415–3425, Jul. 2018.

[18] Y. C. Son, S.-J. Jang, and R. D. Nasrabadi, "Permanent magnet AC motor systems and control algorithm restart methods," U.S. Patent 8 054 030 B2, Nov. 8, 2011.

[19] T. Horie and K. Kondo, "Experimental study on a restarting procedure at coasting condition for a rotational angle sensorless PMSM," *IEEJ J. Ind. Appl.*, vol. 3, no. 2, pp. 131–137, 2014.

[20] T. Yamakawa, S. Wakao, K. Kondo, T. Yoneyama, S. Taniguchi, and S. Mochizuki, "Starting procedure of rotation sensorless PMSM at coasting condition for railway vehicle traction," *Electr. Eng. Jpn.*, vol. 169, no. 2, pp. 56–63, Nov. 2009.

[21] S. Taniguchi, S. Mochiduki, T. Yamakawa, S. Wakao, K. Kondo, and T. Yoneyama, "Starting procedure of rotational sensorless PMSM in the rotating condition," *IEEE Trans. Ind. Appl.*, vol. 45, no. 1, pp. 194–202, Jan. 2009.

[22] K. Lee, S. Ahmed, and S. M. Lukic, "Universal restart strategy for high-inertia scalar-controlled PMSM drives," *IEEE Trans. Ind. Appl.*, vol. 52, no. 5, pp. 4001–4009, Sep. 2016.

[23] T. C. Lin and Z. Q. Zhu, "Sensorless operation capability of surface-mounted permanent-magnet machine based on high-frequency signal injection methods," *IEEE Trans. Ind. Appl.*, vol. 51, no. 3, pp. 2161–2171, Jun. 2015.

[24] S. Kim, J.-I. Ha, and S.-K. Sul, "PWM switching frequency signal injection sensorless method in IPMSM," *IEEE Trans. Ind. Appl.*, vol. 48, no. 5, pp. 1576–1587, Sep. 2012.

[25] S.-C. Yang and R. D. Lorenz, "Comparison of resistance-based and inductance-based self-sensing controls for surface permanent-magnet machines using high-frequency signal injection," *IEEE Trans. Ind. Appl.*, vol. 48, no. 3, pp. 977–986, May 2012.

[26] G. Xie, K. Lu, S. K. Dwivedi, J. R. Rosholm, and F. Blaabjerg, "Minimum-voltage vector injection method for sensorless control of PMSM for low-speed operations," *IEEE Trans. Power Electron.*, vol. 31, no. 2, pp. 1785–1794, Feb. 2016.

[27] J.-I. Ha, K. Ide, T. Sawa, and S.-K. Sul, "Sensorless rotor position estimation of an interior permanent-magnet motor from initial states," *IEEE Trans. Ind. Appl.*, vol. 39, no. 3, pp. 761–767, May 2003.

[28] S. Medjmadj, D. Diallo, M. Mostefai, C. Delpha, and A. Arias, "PMSM drive position estimation: Contribution to the high-frequency injection voltage selection issue," *IEEE Trans. Energy Convers.*, vol. 30, no. 1, pp. 349–358, Mar. 2015.

[29] J.-I. Ha, S.-J. Kang, and S.-K. Sul, "Position-controlled synchronous reluctance motor without rotational transducer," *IEEE Trans. Ind. Appl.*, vol. 35, no. 6, pp. 1393–1398, Nov./Dec. 1999.

[30] K. Lee, S. Ahmed, and S. M. Lukic, "Restart strategy for scalar (V/f) controlled synchronous reluctance machine driving a high-inertia load," *IEEE Trans. Ind. Appl.*, vol. 55, no. 4, pp. 3834–3841, Jul. 2019.

[31] K. Lee and S. M. Lukic, "Restart strategy for scalar controlled synchronous reluctance machine driving a high-inertia load with a single DC-link current sensor," in *Proc. Int. Conf. Power Electron. (ECCE) Asia*, May 2019, pp. 1286–1292.

KIBOK LEE (Member, IEEE) received the B.S. and M.S. degrees in electrical engineering from Korea University, Seoul, South Korea, in 2005 and 2007, respectively, and the Ph.D. degree in electrical engineering from North Carolina State University, Raleigh, NC, USA, in 2016.

From 2007 to 2011, he was a Research Engineer with LG Electronics Research and Development Center, Seoul. From 2016 to 2018, he was a Senior Motor Control Engineer with the General Motors Powertrain Center, Pontiac, MI, USA. He is currently an Assistant Professor with the Department of Mechatronics Engineering, Incheon National University, Incheon, South Korea. His current research interests include motor drives, power conversion systems, and wireless power transfer systems.

HEONYOUNG KIM (Student Member, IEEE) received the B.S. and M.S. degrees in electrical engineering from Korea University, Seoul, South Korea, in 2013 and 2015, respectively. He is currently pursuing the Ph.D. degree in electrical engineering with North Carolina State University, Raleigh, NC, USA. His research interests include high-frequency motor drives and *dv/dt* filter design.

SRDJAN M. LUKIC (Senior Member, IEEE) received the Ph.D. degree in electrical engineering from the Illinois Institute of Technology, Chicago, IL, USA, in 2008. He is currently an Associate Professor with the Department of Electrical and Computer Engineering, North Carolina State University, Raleigh, NC, USA, where he also serves as the Distributed Energy Storage Devices Subthrust Leader of the National Science Foundation Future Renewable Electric Energy Delivery and Management (FREEDM) Systems Engineering Research Center. His current research interests include design and control of power electronic converters and electromagnetic energy conversion with application to wireless power transfer, energy storage systems, and electric automotive systems. He serves as an Associate Editor of the IEEE TRANSACTIONS ON TRANSPORTATION ELECTRIFICATION. He has served as a Guest Editor for the special section of the IEEE TRANSACTIONS ON INDUSTRIAL ELECTRONICS on Energy Storage Systems—Interface, Power Electronics, and Control. He was a Distinguished Lecturer with the IEEE Vehicular Technology Society, from 2011 to 2015.

. . .